ISSN: 0067-2904

Validating and Assessing the Print-grammetry method - Reproducibility of 3D Features without Field Works

Mohammed R. Falih*, Fanar M. Abed
Surveying Engineering Department, College of Engineering, University of Baghdad, Baghdad, Iraq

Received:17/10/2024 Accepted: 24/ 1/2025 Published: 28/2/2026

Abstract

Aerial photogrammetry offers the insights necessary to guide projects, and it is a powerful tool for civil and construction engineers. Using rapid computer vision (C.V.) photogrammetry development, structure from motion (SfM) algorithms became an integral part of the photogrammetry technique. Integrating SfM algorithms and photogrammetry through the so-called print-grammetry technique allows the creation of real-world 3D models, avoiding the need for site visiting and fieldwork. This study aims to assess three print-grammetry scenarios for capturing screen images from the Google Earth (GE) Pro using various camera orientation settings to follow these advancements. Images were captured automatically, allowing the user to set the image size and interval time for screen image capturing. The outcomes model for individual scenarios was classified into three categories (buildings, corridors, grass area) and inspected with a reference 3D model generated by photogrammetry. The results show that images captured from the nadir have a minimal mean and standard deviation across classes of the outcome models. However, images captured at a 45° orientation angle in the north-south path and a 0° orientation angle in the east-west path achieve average values compared to other scenarios. The outcomes indicated that capturing oblique images obtained the highest STD values compared to vertical images, demonstrating a lower accuracy level than scenarios captured by truly vertical images. On the other hand, reference point errors and point density provide essential insights in evaluating individual scenarios. Scenario *A* presents the lowest rate of errors; however, scenario *B* dominates in point density and is therefore suitable for large areas due to more data collection in a shorter period. Scenario *C*, on the other hand, displays a high error rate and low score, which reduces accuracy and efficiency.

Keywords: Photogrammetry, Object structure, Structure from Motion, Accuracy analysis, Data Validation.

تقييم كفاءة المسح التصويري بطريقة الـ *Print-Grammetry* – إعادة انتاج العوارض الارضية ثلاثية الأبعاد بدون أعمال ميدانية

محمد رحمن فالح*, فنار منصور عبد
قسم هندسة المساحة ، كلية الهندسة ، جامعة بغداد ، بغداد ، العراق

* Email: mohammed.r@coeng.uobaghdad.edu.iq

الخلاصة

يعد التصوير المساحي الجوي أداة فعالة للمهندسين المدنيين ومهندسي البناء لكونه يوفر الرؤى اللازمة لتوجيه المشاريع. مع التطور السريع في التصوير المساحي لرؤية الكمبيوتر (C.V.)، أصبحت خوارزميات البنية من الحركة (SfM) جزءًا لا يتجزأ من تقنية المسح التصويري. يتيح تكامل خوارزميات SfM والمسح التصويري من خلال ما يسمى بتقنية ال Print–grammetry إنشاء نماذج ثلاثية الأبعاد في الواقع الحقيقي، مما يتجنب الحاجة إلى زيارة الموقع وإجراء العمل الميداني. لمواكبة هذه التطورات, تهدف هذه الدراسة إلى تقييم ثلاثة سيناريوهات منفردة لل Print–grammetry في التقاط صور الشاشة من Google Earth Pro. (GE)بأستخدام اعدادات مختلفة لأتجاهات الكاميرا. تم التقاط الصور تلقائيًا مما يسمح بتعيين حجم الصورة والفاصل الزمني لالتقاط صور الشاشة. تم تصنيف نموذج النتائج لكل سيناريو إلى ثلاث فئات (المباني والممرات ومنطقة العشب) وتم فحصه باستخدام نموذج مرجعي ثلاثي الأبعاد تم إنشاؤه بواسطة المسح التصويري. تسلط النتائج الضوء على أن الصور الملتقطة مباشرة فوق منطقة الدراسة بزاوية 0 درجة من النظير لها أدنى حد من المتوسط والانحراف المعياري عبر فئات نماذج النتائج. السيناريو B، الذي يلتقط الصور بزاوية 45 درجة في المسار بين الشمال والجنوب و0 درجة في المسار بين الشرق والغرب، يحقق قيمًا متوسطة مقارنةً بالسيناريوهات الأخرى. أشارت النتائج ان التقاط الصور المائلة حصل على اعلى قيم للانحراف المعياري مقارنة بالصور الرأسية، مما يدل على مستوى دقة أقل من السيناريوهات الملتقطة صوراً رأسية تماماً. ومن ناحية أخرى، توفر أخطاء النقطة المرجعية وكثافة النقطة رؤى مهمة في تقييم كل سيناريو. يقدم السيناريو A أقل الأخطاء، ومع ذلك، يهيمن السيناريو B على كثافة النقطة وهو مناسب للمناطق الكبيرة من خلال جمع المزيد من البيانات بسرعة. يعرض السيناريو C معدل خطأ مرتفعًا مما يقلل من الدقة والكفاءة.

1. Introduction

Engineers must look at the environment around them and turn unrealized potential, such as undeveloped land or dilapidated building structures, into actual initiatives to promote social advancement [1]. The 3D Modelling techniques, including image-based photogrammetry, allowed civil and construction engineers to transform real-world objects into digital forms [2][3]. This is achieved by providing a detailed, realistic photo visualization of these objects by extracting their geometric properties and texture for successful decision-making [4]. The digitization process of real-world objects can provide engineers with valuable information about object structures for more crucial decision-making in engineering projects [5]. Today, the majority of digital modeling methodologies are based on the most advanced remote sensing technologies, such as image-based and range-based (i.e., digital photogrammetry and laser scanning) [6][7]. Due to the proliferation of aerial platforms such as unmanned aerial vehicles (UAVs) and professional high-quality cameras, photogrammetry has become the most popular 3D modeling technique nowadays [8].

Structure from Motion (SfM) photogrammetry is the norm in the photogrammetric domain nowadays, where the Computer Vision (CV) process involved in the extraction of 3D geometry from a set of overlapping, un-calibrated, and un-referenced 2D images [9]. In this process, the 3D re-constructed geometry of the scene emerges following several CV algorithms where no specific geometric conditions are required in the source photos, such as camera positions, orientation, scaling, etc. [10]. In contrast, traditional photogrammetry (TP) is a long-established process requiring semi-parallel 2D images, accurate approximation of camera positions, and prior knowledge of the exposure orientation, usually obtained through control information [11]. The camera calibration process is essential in TP to compensate for the camera parameters and image distortion to represent the 3D scene accurately [12]. Therefore, TP is considered a time-consuming and semi-automatic process compared to SfM photogrammetry [10]. The SfM Photogrammetry is not limited to 2D image matching and

filtering through the SfM algorithms, but it extends to include the process of extracting, triangulating, and densifying the 3D data [13]. This is usually obtained in a later stage process following the Multi-View Stereo (MVS) algorithm [14]. Therefore, the complete processing pipeline of the CV Photogrammetric process is technically referred to today as SfM-MVS photogrammetry [9].

Print-grammetry is an advanced data capture method based on SfM-MVS photogrammetric concepts to re-produce a realistic 3D geometric representation of the topographic features without fieldwork [15]. Hence, this research mainly focuses on the feasibility of this approach and analyses the impact of specific data acquisition parameters (angle orientation and data capture direction) on the geometric quality outcomes obtained from the ground objects based on print-grammetry methodology. The paper analyses different data-capturing scenarios to demonstrate the efficiency of the Print-grammetry method for users in the end engineering process.

2. Theoretical Background

SfM-MVS Photogrammetry is a method that uses 2D photos to produce intricate 3D models [16]. Figure 1 illustrates the fundamental SfM-MVS Photogrammetric workflow, including feature detection, data filtering, geometric identifications, scaling and refinement, and MVS matching. Print-grammetry is one of the modeling methodologies based on SfM-MVS photogrammetry but built explicitly on Google Earth's (GE) 3D imagery service, where 3D data is available [17]. It is a new image-based modeling method motivated by technological advancements in the CV that incorporates the GE engine and SfM-MVS photogrammetric pipeline to extract 3D geometry of topographic objects for diverse applications [18]. Print-grammetry was built to capture high-resolution images from GE using a 4K monitor screen to build a 3D Virtual Field Environment (VFE) and facilitate digitizing the real-world objects to aid researchers and professionals in their projects [19]. It is formulated to provide a practical tool to analyze physical objects without needing physical access to reach the site and avoid any field work [15]. Print-grammetry includes four mandatory stages to be considered before establishing any project to be structured on this methodology [18], Figure 2.

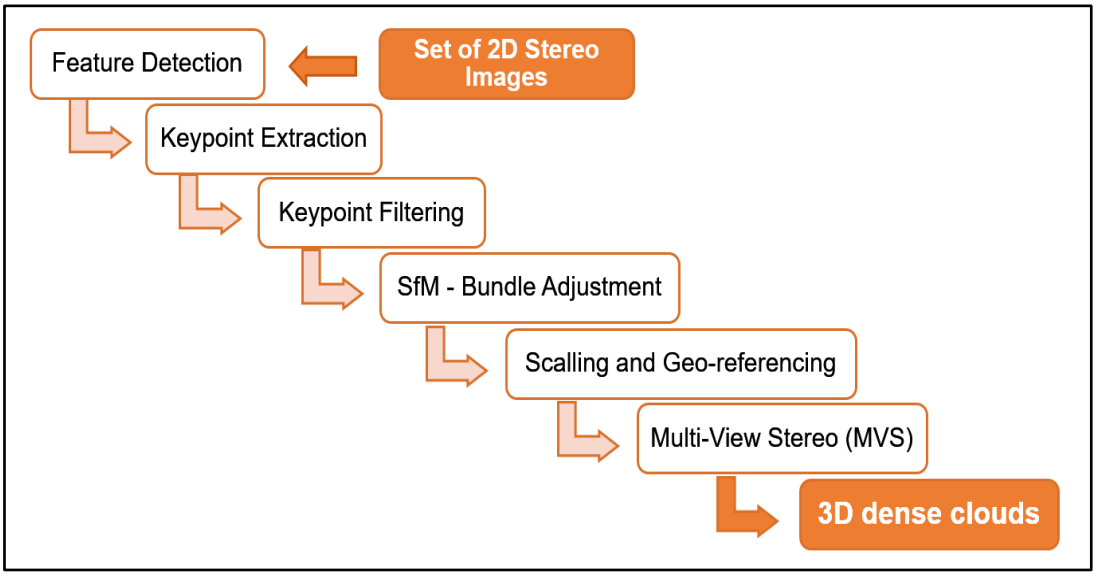

Figure 1: The fundamental workflow of SfM-MVS Photogrammetry.

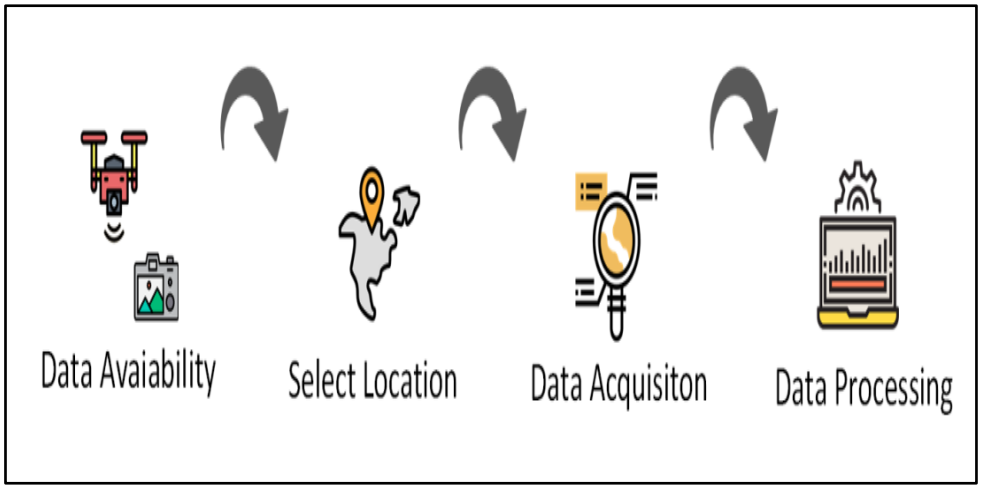

Figure 2: The work frame stages in Print-grammetry [19].

The first step in this processing chain is to ensure the availability of the reference topographic data to validate the Print-grammetry results in later stages and verify the methodological potential [15]. Then, it is essential to check the 3D coverage of the selected location of the targeted study area through the 3D data Imagery service in the GE Pro to verify the quality of the captured images and the availability of the depth geometric information [17]. It is worth mentioning that 3D data imagery is a 3D data service provided by GE since 2009, obtained initially from high-resolution aerial photographs captured by drones. This service mirrors the entire Earth and provides a virtual 3D flight simulator of our planet with a realistic image source for end users at any viewing angle or latitude [15]. This 3D imagery service has been extended to include hundreds of cities in more than 40 countries by 2016 [18]. The third stage in print-grammetry methodology is data acquisition, which is considered the workflow's main and most challenging step. This includes multiple manual steps such as camera setup, flight planning, ground control selection, scaling consideration, and image capturing process from the screen monitor [19]. To fulfill the required accuracy in the geospatial positioning of the end products, multiple considerations should be considered when designing the flight planning [20], Equation 1.

$$\sigma_{XYX} = \left(q * S * \sigma_{xy}\right)/\sqrt{K} \quad (1)$$

Where σ_{XYX} represents the expected accuracy in the extracted 3D point clouds, q is the flight plan design factor, which shows the strength of the camera station design through keeping the B/H ratio > 0.5, S is the image scale factor, σ_{xy} is the accepted error in the re-projected error obtained from the SfM process, while K is the number of images captured per station.

When these parameters are correctly specified, the data-collecting process can accomplish the desired outcome by producing the anticipated geospatial precision of the final products using the Print-grammetry technology [21]. After data is collected, SfM-MVS photogrammetry is used to process the information and create realistic 3D renderings of the case study objects, which should be sufficiently reliable [22].

3. Previous Works in Print-grammetry Method

The print-grammetry method was first established in 2016 by [17], who presented a practical work frame methodology on how to re-extract the 3D geometry of ground features by capturing images from GE 3D models screen window and processing these images following the SfM-MVS photogrammetric approach. The study aimed to measure the discrepancies between the GE-based SfM models and the reference LIDAR models to validate the accuracy level of the presented methodology. The project goal was to present an advanced approach to limit the overall cost and the required resources in standard

photogrammetry and avoid fieldwork efforts. The method can also be used when limited access to specific locations, moderate accuracy requirements, and low computing facilities may fail to run large sets of images through the popular SfM process [18].

In the [17] study, they used three case studies to analyze ground coverage diversity by selecting one case study in Japan and two in the USA to assess the presented method over different topographic properties, including urban and natural landscape environments. Oblique screen images have been generated from the oblique video recorded to the ground through the GE window to reconstruct the selected scene's depth information. Japan's and the USA's case studies used a 45° camera orientation setting to capture the images following a simulated flight plan of parallel lines flown at 300 m and 1000 m, respectively. The results showed a successful application of the data-capturing process and a successful SfM modeling implementation. However, the accuracy of the obtained 3D point clouds showed a significant instability between the GE-based SfM model and the reality in the horizontal and vertical directions reaching 100 m. They claimed that the limited camera perspective and quality can highly affect the results from the positional accuracy of the final products. However, camera perspective and orientation have a more significant role.
Later, [19] presented an extended study of [17] by providing a detailed technical workflow of Print-grammetry methodology for Virtual Reality (VR) applications. They built on [17] suggestions to improve the quality of the captured 2D images to ensure the best geometric and visual data quality extracted from GE. They claimed the possibility of delivering high-quality geometric results from the print-grammetry method if four distinct variables are considered during the flight planning and data acquisition stage. These are: increasing the resolution of the captured images by taking the images at the highest Level of Detail (LOD) possible, capturing the images from a 4K screen monitor, capturing the images from GE at various directions and perspectives angles, and selecting homogeneous distribution of reference ground targets for geo-referencing requirements.
To verify the impact of these conditions, they implemented the method in the Half Dome in Yosemite Vally- California/USA, to assess the validity of the vast change in topographic relief. The image acquisition phase was implemented using Greenshot software (https://getgreenshot.org/) and a 4K monitor to deliver images with 8.3 MB resolution. The flight plan was designed with the highest LOD at an average flying altitude of 500 m using parallel flight lines to ensure the maximum overlap coverage with a 45° camera orientation setting. The plan was set to include back-and-forth flight directions to fulfill high-quality requirements and increase ground coverage. Moreover, [19] has set the scale of the extracted 3D data based on the homogeneous spaced selection of well-defined GCPs in the UTM-based WGS84 coordinate system. The results showed significant improvements in accuracy standards in natural landscapes compared to those delivered from the [17] study. They also claimed an improvement in the precision level, reaching 91.31% of the overall coverage area and eliminating the differences between the GE-based SfM model and the reference model to less than 10 m in complex relief areas.

In 2020, [15] investigated the print-grammetry method in different case studies to analyze the methodology potential for geological studies and outcrop 3D modeling. Following this method, they generate the Virtual Outcrop Model (VOM) and Digital Outcrop Model (DOM), crucial decision-making products for multiple engineering projects such as data mining in oil or gas. They demonstrated the potential of this approach to extract the DOM as a feasible alternative to the expensive LIDAR technology and UAV-based aerial photogrammetry, which have limited usage in countries with restricted regulations on flying altitude allowance and inaccessibility to particular regions. Therefore, print-grammetry would be a perfect option to extract a 3D photorealistic representation of the ground coverage from

GE, as the latter did not provide any export tool to transfer the 3D data to third-party software for post-processing and data analysis.

Hereby, [15] has applied his methodology on selected study sites in the USA of severe topographic relief to analyze the quality of print-grammetry products in challenging geological sites. They eliminate errors inherent in the SfM-based 3D extracted data using the SOR noise removal tool in the CloudCompare (CC) environment before the registration application with the reference LIDAR data in CC using the Cloud to Cloud (C2C) tool. This process has returned with a 4.4 m total accuracy based on the selected GCPs in the first case study. However, the vegetation in the valley case study has represented errors between 5 and 15 m, which decreases the overall accuracy level. After eliminating the outlier points, the DOM was extracted from 6,975,566 triangles and later exported for public visualization and downloading from the Sketchfab platform [15]. In the second case study, they delivered 1.38 m RMSE over the selected GCPs where no vegetation was present, and the surface was much smoother than the surface in the first case study. These results were obtained from the [15] study when they maintained the data acquisition conditions proposed by [19]. However, they increased the quality of the captured images by using a higher-resolution screen monitor.

Recently, [18] presented an assessment study to analyze the impact of different flying altitudes in print-grammetry methodology on geometric positioning accuracy in an urban site in a residential neighborhood in Boston, USA. They used a 4K resolution monitor to capture the images (3840 × 2160) pixels. Two simulated fight missions were performed to acquire high-resolution images at 80 m and 250 m flying heights using double grid plans to extend the ground coverage. They set the camera exposure to be 30° tilted from Nadir, delivering 272 and 120 images at 80 m and 250 m flying altitudes, respectively. They manually draw the flight lines and the positions of the exposure stations using the path drawing tool in GE to maintain the required LOD of the ground objects. They extracted 23,299,227 and 4,256,074 point clouds in both flight missions following a successful SfM-MVS application. Following SOR data cleaning, 1.183 m and 1.211 m RMSE were delivered for 80 m and 250 m flight missions, respectively. They found that the data precision is decreased whenever the flying altitude increases. However, the noise data can be removed when the empirical noise removal approach is implemented following the resulting LOD.

The above review studies were compiled based on the Scopus dataset (http: //www.scopus.com) search to keep up to date with all available related studies. Following the available literature search, the presented research aims to assess the role of flight planning and camera orientation setup in the print-grammetry methodology and analyze their impact on the 3D geometric quality of the final derivable using different camera settings. It also provides an automatic image capture routine from the screen monitor to avoid the exhaustive manual process in the Print-grammetry workflow.

4. Study Location

This research was conducted within the borders of the College of Engineering, including part of the University of Baghdad (UOB) campus, situated on the Al-Rusafa side of the Al-Jadrriya compound in the heart of Baghdad city. The UOB campus is encircled by the Tigris River on three sides, making it a peninsula which is situated at 33° 16′ 24.92″ N and 44° 22′ 30.10″ E in geographic coordinates system. The test region covers an area of approximately 55000 m^2 with a ground-level elevation of 39 m above mean sea level. The region is an urban site with naturally occurring and artificially created land-cover characteristics, see Figure 3.

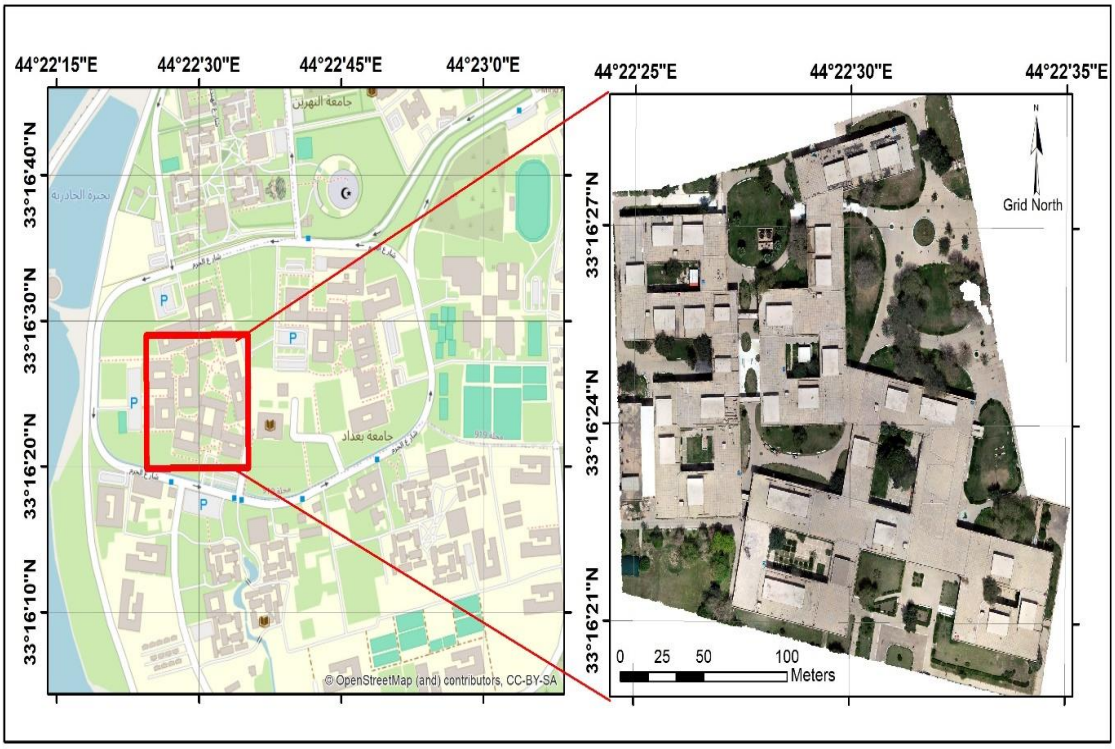

Figure 3: Study area location in the UOB campus.

5. Methodology

As previously mentioned, printgrammetry consists of four mandatory stages, including checking the 3D coverage of the selected case study through the 3D data imagery service in the GE. However, in this research, the study area was selected to be in Baghdad, Iraq, where the GE provides no coverage of the 3D imagery service in this zone. Alternatively, the 3D imagery coverage was obtained from previous work in the same study site based on UAV Very High Resolution (VHR) images; see [23] for more details. This site's generated 3D virtual reality data was uploaded by [23] through the GE Pro for public usage. Further, the raw 2D image data was also available in their original high-resolution format, which was collected by a drone for the same study site. This research considered it a reference to validate the extracted Printgrammetry-based model.

The approach presented herein was based on [18] recommendations when a UAV platform or dataset is not obtainable for a particular endeavor site. Therefore, this section outlines the presented methodology, which is based on collecting images of different camera settings for the 3D data coverage extracted by [28] from the screen window of the GE Pro platform following the print-grammetry workflow. The methodology assesses the accuracy and efficiency of the extracted ground objects through three distinct data-capturing scenarios (labeled as A, B, and C). This is based on generating standalone Printgrammetry-based 3D models from the collected screenshot images captured based on an automatic in-house routine from GE using multiple overlapping plans. The plans are based on three camera orientation settings to check their impact on the ground objects' quality and geospatial positioning through the Print-grammetry approach.

To apply the proposed methodology, several tools were utilized to meet the objectives of this study:

- AutoCAD Civil 3D: Used to create a mission plan based on an 85% overlap and 70% end lap/side lap coverage.

- IrfanView: Used to automatically capture screenshots of the interest area from the GE Pro monitor window.
- Agisoft Metashape: Used to process the images and generate the 3D Print-grammetry-based models.
- Google Earth Pro: Used to view the area of interest in 3D coverage.
- CloudCompare: Used for 3D point cloud data analysis and model inspection.

5.1 Data Acquisition

Data acquisition is crucial to successfully implementing the print-grammetry approach [18]. The data capturing plan and camera acquisition settings can significantly impact the accuracy of the product results [13][24]. In this research, three different scenarios were employed to capture images of the designated area for 3D model generation:

- Scenario A: Images were captured with a 0° camera orientation angle from the nadir in both East-West and North-South data capturing paths.
- Scenario B: Images were captured with a 0° camera orientation angle in the North-South path and at 45° angle in the East-West path.
- Scenario C: Images were captured with a 45° camera orientation angle from the nadir in both North-South and East-West data capturing paths.

The mission planning of these scenarios was based on a critical analysis of previous studies' findings [13] to analyze the impact of image acquisition geometry and flight planning path on the derived 3D products [25][26][24]. Mission planning represents an essential process in photogrammetry to obtain accurate and satisfying results. It encompasses various factors such as ground coverage area, focal length, sensor dimensions, flight altitude, image overlap, and line spacing [27]. Reconstruction with adequate coverage and minimal gaps in the data is ensured by using 80% to 90% forward overlap and 60% to 70% side lap overlap, according to literature, for best products based on Structure from Motion-Multi-View Stereo (SfM-MVS) photogrammetry [28][29].

Several factors are considered to determine the distance between adjacent flight lines, including the flying height (H), image coverage distance (G), and the required end lap/side lap coverage percentage. As the GE screen window does not function as a regular camera and lacks a focal length value like any camera lens, image coverage distance (G) was computed based on measurements from the screen using the ruler tool in GE, Equations 2 and 3. The height and width of the image coverage are found to be 58.0 m and 109.3 m for the study area, respectively. The flight altitude was 100 m, while the forward and side overlap amount was 85% and 70%, respectively. To calculate the distance between adjacent flight lines (along-track and cross-track), Equations (4) and (5) are applied [11].

$$G_h = S * Cfh \quad (2)$$

$$G_w = S * Cfw \quad (3)$$

$$B = (1 - endlap) * G_w \quad (4)$$

$$\mathrm{W} = (1 - \text{side lap}) * G_h \quad (5)$$

Where G_h is the image coverage distance in the along-track direction, G_w is the image coverage distance in the cross-track direction, S is the image scale number, Cfh is the window frame height, Cfw is the window frame width, B represents the image base distance, and W is the lateral advance distance per strip.

From the above equations, the distance between flight lines was computed to be 11.6 m and 32.79 m for along-track and cross-track, respectively. Later, AutoCAD Civil 3D was used to create a mission plan based on the computed overlap percentages. The flight path line was modeled in AutoCAD as a polyline and then exported in KMZ file format to the GE

environment. The KMZ file was imported into GE Pro, which was used to visualize the mission plan and ensure the complete coverage of the area of interest, Figure 4.

To eliminate manual interaction from the user in the presented methodology, images are automatically captured using IrfanView software. IrfanView is set up to capture screenshots at a specific interval based on the designed mission plan. This was applied every 1.5 seconds to maintain the overlapping coverage while the GE Pro app ran in the background. The screenshots were saved in tiff format (~ 4.5 MB) in a specified folder for later post-processing. Figure (5) illustrates the data capturing settings used in IrfanView.

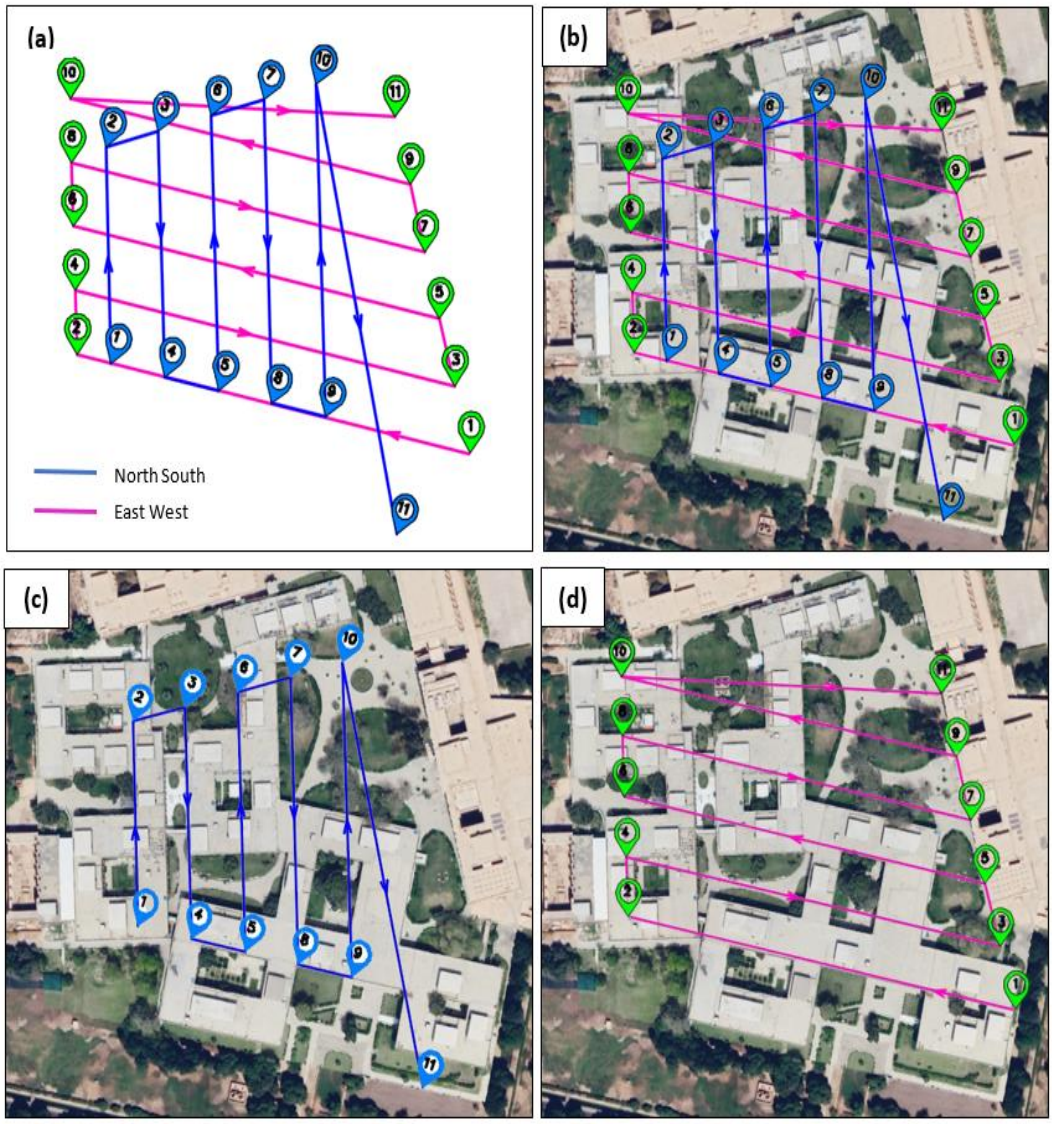

Figure 4 : Flight plan path configuration; (a) represents East-West and North-South paths produced in AutoCAD Civil 3D; (b) flight path used in scenarios A and C (North-South and East-West); (c) flight path used in scenarios B (North-South); (d) flight path used in scenarios B (East-West).

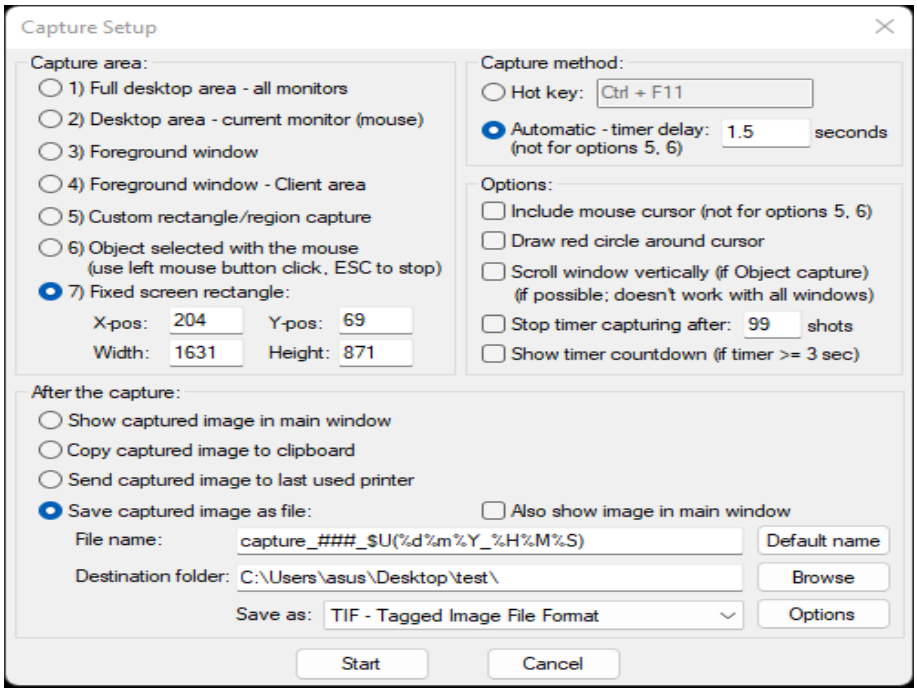

Figure 5 : The settings of the camera capturing used in IrfanView.

5.2 Data Processing

The captured screenshots were imported into the SfM work frame for post-processing, where the images were firstly aligned based on the SfM application, outliers and noise were removed, and the dense 3D point clouds were generated following MVS geometry. The 3D point clouds of the individual standalone scenario were classified into three categories: buildings, corridors, and grasses, based on their visual characteristics (no further classes were generated to fulfill the main research objective). This classification was applied automatically based on Agisoft Metashape. However, the results were manually modified based on visual analysis. The selected features were then assigned to their respective classes.

The print-grammetry-based 3D models generated following scenarios A, B, and C were analyzed and compared to the reference-based model (R) to check the validity and highlight flight path and camera orientation impacts on the positional accuracy. The cloud-to-cloud distance (C2C) tool was utilized for the metric comparison from CC. The classified datasets' mean and standard deviation were calculated and analyzed for individual scenarios to evaluate the precision and noise level inherent within the extracted point clouds. These statistical parameters were extracted based on the best Gaussian fitting function within the CC environment. Later, Root Mean Square Errors (RMSE) are computed according to the reference dataset to assess the resulting ground accuracy.

6. Results and Discussion

After configuring the required settings in the IrfranView, approximately 350 images were captured for individual scenarios at a resolution of 1631×871 pixels. The images were subsequently exported to Metashape for post-processing, where the sensor size was set to a full-frame sensor (36×24 mm) to determine the corresponding pixel size and focal length values. Setting a precise pixel size and focal length are crucial factors for achieving accurate camera calibration parameters, as camera calibration represents an essential step in the photogrammetry workflow. Following the SfM-MVS work frame process, the generated point clouds are analyzed to eliminate outlier observations in the three extracted standalone models.

The 3D individual Printgrammetry-based models were categorized into three distinct classes - buildings, corridors, and grasses - based on their visual characteristics to facilitate an accurate comparison with the reference model within each category. In this regard, all buildings were included in the classification process, while only selected portions of the corridors and grasses were chosen to avoid oversampling for evaluation purposes. The results of the classification process across the selected categories are presented in Figure 6.

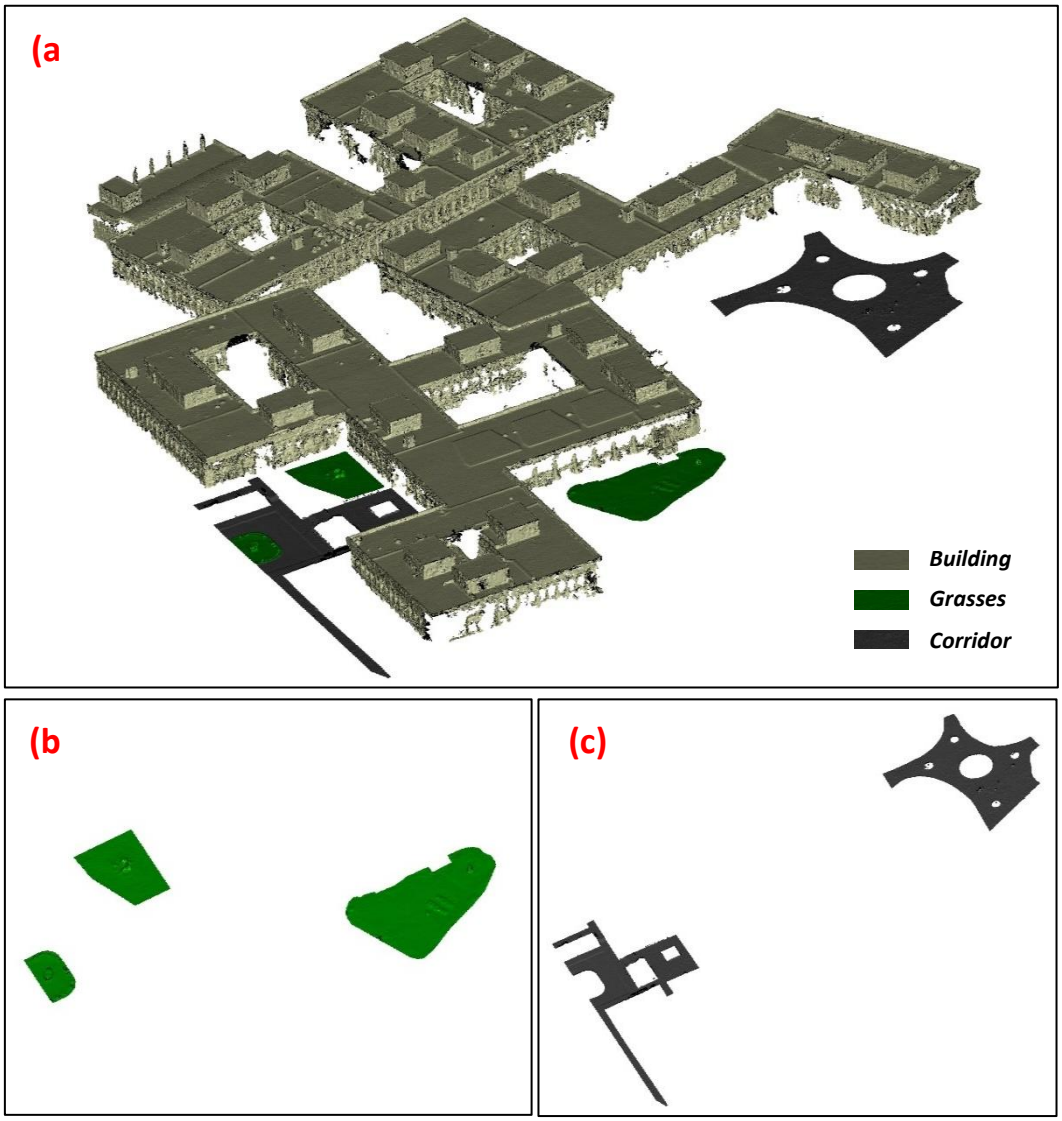

Figure 6 : Classification results: (a) the entire classification for each category of the model; (b) grasses class enlarged; (c) corridors class enlarged.

Figure 7 shows the accuracy analysis based on the Gauss fitting function of the building class in the three generated print-grammmetry models to assess the quality of the extracted models. In this analysis, the mean and the standard deviation were computed by comparing the generated 3D printgrammetry models obtained from data-capturing scenarios A, B, and C with the reference model, respectively.

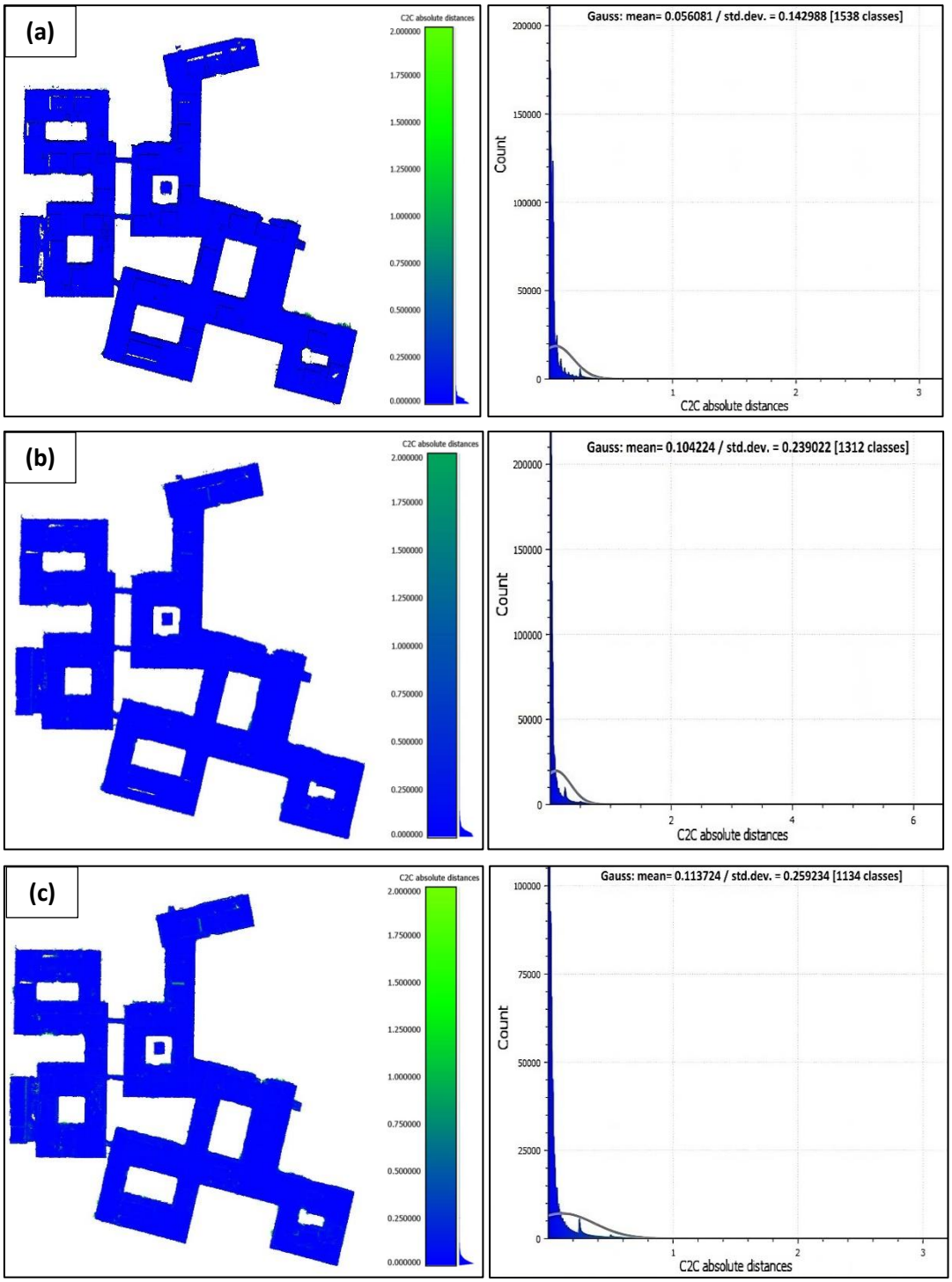

Figure 7 : Accuracy analysis of the generated building class from scenarios A, B, and C.

From this figure, one can evaluate how the camera orientation impacts the quality of the generated 3D point cloud by comparing the standard deviation values obtained from scenarios A and C as the flight route is maintained fixed, Figure 7. When the camera orientation setting is in the Nadir direction, scenario A's standard deviation was 14 cm, showing a substantial improvement over scenario C. The standard deviation in scenario C, where the camera position was set to 45°, went as high as 25 cm. The assessment was also based on density analysis performed on the extracted model individually, Table 1 for the building class. The Point density represents the number of points per area unit, which was analyzed to gain insight into the level of detail (LOD) present in each of the extracted 3D

models, Table 1. The investigation demonstrates how camera direction can reduce dataset resolution through a discernible fall in the number of point clouds in oblique views.

Table 1: Density analysis of the building class.

	Density (pt/m^2)		
Model (Building Class)	**Total No. of Points**	**Mean**	**Std. dev.**
Reference	13918513	317	**91**
Scenario A	2365343	65	**13**
Scenario B	1721009	42	**8**
Scenario C	**1283821**	**30**	**6**

In contrast, the results of scenario B's standard deviation with those of scenario C reveal a rise in standard deviation values in C compared to B, Figure 7. The camera angle in these two scenarios was designed to be vertical and oblique coverage in B and entirely oblique coverage in C. The flight path direction was identical in both the B and C cases, doubling the coverage. Comparing scenario B to scenario C, which only provides oblique coverage, one can see the benefits of combining vertical and oblique camera orientation options in a single flight plan. This is also demonstrated through the standard deviation values in density analysis highlighted in Table 1, where the oblique camera orientation settings can potentially increase the extracted number of points and the overall resolution when integrated into normal images compared to only oblique coverage in C, Table 1. Contrarily, the precision analysis results shown in Table 2 reveal high outlier values in the building class compared to corridor and grass classes in any scenario. However, when the grass class is not considered, this shows how building heights and shading factors can lead oblique coverage to produce erroneous points by comparing standard deviation findings from buildings with those from corridor class. However, compared to other scenarios in all specified classes, the data still indicate that scenario A had better standard deviation outcomes. These results were enhanced by SOR noise removal to remove erroneous measurements before accuracy analysis.

Table 2: Precision analysis of the extracted Print-grammetry models per class.

Scenarios	**Buildings**		**Corridors**		**Grass**	
	Mean (m)	**STD (m)**	**Mean (m)**	**STD (m)**	**Mean (m)**	**STD (m)**
Scenario A	0.056081	0.142988	0.026073	0.062879	0.014005	0.024315
Scenario B	0.104224	0.239022	0.0367763	0.080563	0.020555	0.048339
Scenario C	0.113724	0.259234	0.046579	0.130814	0.025329	0.052551

Later, the accuracy assessment of the extracted Printgrammetr-based models was analyzed based on selective ground-truth reference points. A quality control test was performed by comparing the results of the control and checkpoints selected in the 3D models with their ground-truth coordinates measured and adjusted following the Global Navigation Satellite System (GNSS) networking adjustment provided by [23]. A visual inspection of the generated models was conducted compared to the referenced model (R), including the calculation of the mean and the standard deviation for standalone scenarios, to provide a qualitative evaluation of the comparative models. These evaluations comprehensively assessed the accuracy and precision of the 3D-generated models. Table 3 summarizes the accuracy analysis applied for individual models extracted from the three scenarios compared to the reference model.

Table 3 : Accuracy analysis of individual Printgrammetry-based models.

Models	Horizontal Error (cm)		Vertical Error (cm)	
	GCPs	Check Points	GCPs	Check Points
Reference	0.554958	1.85178	0.104819	**1.60167**
Scenario A	0.173737	2.125250	0.154268	**5.028080**
Scenario B	0.399823	4.146950	0.214978	**5.197060**
Scenario C	**0.304772**	**5.232630**	**0.238554**	**5.660490**

The results shown in Table 3 show that the extracted reference model's accuracy was 0.55 cm and 0.15 cm in the horizontal and vertical directions, respectively, based on the raw UAV photos. The GCPs error provides essential information about the accuracy of each scenario. The 3D model created by scenario A was the most accurate compared to the reference model since it has the lowest control and checkpoint inaccuracy in horizontal and vertical dimensions. However, scenario B has the highest number of points but a lower accuracy level than A, which suggests that this scenario may be more suitable for capturing larger areas, as it captures more data points in a shorter time. The lowest number of points and maximum GCPs inaccuracy for Scenario C suggest that this scenario may not be the most precise or effective method for collecting data for 3D modeling in urban sites. The results indicate that capturing Nadir images from directly above the area (scenario A) is the most accurate way to build a 3D model. However, capturing images at an oblique angle can still lead to a relatively accurate model, especially when combined with Nadir images (scenario B), because Nadir images guarantee uniform resolution throughout the image and reduce distortion [30]. However, combining oblique with Nadir images is more beneficial over high buildings and complex terrain as it helps to reduce blind areas and provide new views. It is essential to consider the trade-offs between accuracy and efficiency, as scenarios that capture more data points may be more suitable for larger areas but may not produce the most accurate models.

7. Conclusions

When there is no access to a site or when a UAV platform or dataset is not available for a certain project, the Print-grammetry approach offers a practical alternative to the average SfM photogrammetric process. The study evaluates the 3D model created using the Print-grammetry method and the GE Pro imaging service platform. The study's objective herein is to evaluate the function of flight planning and camera orientation setup in the print-grammetry process and to examine how different camera settings affect the 3D geometric quality of the final derivable. Additionally, it provides a routine for alternate 3D data utilization when GE coverage for the 3D imagery service is unavailable and automatically takes images from the screen monitor to minimize the need for the time-consuming manual step in the print-grammetry procedure.

The study's findings contrast three scenarios—A, B, and C—for taking screen photos from GE Pro and converting them into a 3D model at the University of Baghdad. Every scenario calls for taking photos from various perspectives. To evaluate the precision and correctness of the retrieved 3D data following ground truth reference targets, the models were compared using statistical analysis to a reference 3D model. The mean and standard deviation were determined for every scenario and type of categorized objects (buildings, hallways, and grassy spaces). For individual scenarios, the control point's inaccuracy and point density are also included in the results. According to the results, the mean and standard deviation values for all categorized items are produced by scenario A, where truly Nadir images were captured at a 0° degree angle in both the east-west and north-south directions. This implies that taking photos directly overhead yields an accurate three-dimensional model. Scenario B's mean and

standard deviation values, which involve integrating Nadir photos with a 0-degree angle in the north-south direction and oblique photos with a 45-degree angle in the east-west direction, are higher than scenario A's. However, they are lower than scenario C, which also entails capturing only oblique photos with a 45-degree angle in both directions. This suggests that while collecting photos directly overhead can yield a more precise 3D model, taking photos with a slanted orientation can still yield one. However, combining oblique and nadir photos should increase accuracy, which significantly depends on the nature of the region of interest and the elevation change of the ground feature, which was not substantial in our research area [31]. It has been found that the 3D model produced by printgrammetry may be used for medium accuracy projects with a range of centimeters to tens of centimeters when using ground truth and reliable GCPs, such as industrial applications. Future studies will, therefore, examine comparable situations over intricate terrain and employ additional camera settings to examine effects under challenging surroundings.

References

[1] A. Mulahusić, N. Tuno, D. Gajski, and J. Topoljak, "Comparison and analysis of results of 3D modelling of complex cultural and historical objects using different types of terrestrial laser scanner," *Surv. Rev.*, vol. 52, no. 371, pp. 107–114, 2020.

[2] D. P. Pocobelli, J. Boehm, P. Bryan, J. Still, and J. Grau-Bové, "Building information models for monitoring and simulation data in heritage buildings," *Int. Arch. Photogramm. Remote Sens. Spat. Inf. Sci. - ISPRS Arch.*, vol. 42, no. 2, pp. 909–916, 2018.

[3] Y. Alshawabkeh, A. Baik, and Y. Miky, "Integration of laser scanner and photogrammetry for heritage BIM enhancement," *ISPRS Int. J. Geo-Information*, vol. 10, no. 5, 2021.

[4] F. Remondino and S. Campana, *3D Recording and Modelling in Archaeology and Cultural Heritage: Theory and Best Practices*, vol. 24, no. 10. 2014.

[5] A. R. Qubaa, A. N. Hamdon, and T. A. Al Jawwadi, "Morphology Detection in Archaeological Ancient Sites by Using UAVs/Drones Data and GIS techniques," *Iraqi J. Sci.*, vol. 62, no. 11, pp. 4557–4570, 2021.

[6] W. Moussa, "Integration of Digital Photogrammetry and Terrestrial Laser Scanning for Cultural Heritage Data Recording," University of Stuttgart, 2014.

[7] M. Mohamed, Z. E. El Din, and L. Qais, "Accuracy Assessment of 3D Model Based on Laser Scan and Photogrammetry Data," *Iraqi J. Sci.*, vol. 62, no. 11, pp. 4195–4207, 2021.

[8] M. A. Mahmood, N. K. Ghazal, and F. H. Mahmood, "Optimizing Spatial Accuracy for Photogrammetric Processing of Drone-based 3D Mapping," *Iraqi J. Sci.*, vol. 65, no. 7, pp. 4124–4138, 2024.

[9] J. L. Carrivick, M. W. Smith, and D. J. Quincey, *Structure from Motion in the Geosciences*, vol. 73, no. 2. John Wiley & Sons, 2017.

[10] X. Wang, F. Rottensteiner, and C. Heipke, "Structure from motion for ordered and unordered image sets based on random k-d forests and global pose estimation," *ISPRS J. Photogramm. Remote Sens.*, vol. 147, pp. 19–41, 2019.

[11] P. R. Wolf, B. A. Dewitt, and B. E. Wilkinson, *Elements of Photogrammetry with Application in GIS*. McGraw-Hill Education, 2014.

[12] J. Kolecki, P. Kuras, E. Pastucha, K. Pyka, and M. Sierka, "Calibration of Industrial Cameras for Aerial Photogrammetric Mapping," *Remote Sens.*, vol. 12, no. 19, 2020.

[13] A. Kyriou, K. Nikolakopoulos, and I. Koukouvelas, "How image acquisition geometry of uav campaigns affects the derived products and their accuracy in areas with complex geomorphology," *ISPRS Int. J. Geo-Information*, vol. 10, no. 6, 2021.

[14] L. W. and L. L. Feiyang Pan, Pengtao Wang, "Multi-View Stereo Vision Patchmatch Algorithm Based on Data Augmentation," *Sensors*, vol. 23, no. 5, 2023.

[15] R. K. Horota *et al.*, "Printgrammetry-3-D Model Acquisition Methodology from Google Earth Imagery Data," *IEEE J. Sel. Top. Appl. Earth Obs. Remote Sens.*, vol. 13, pp. 2819–2830, 2020.

[16] F. Brandolini and G. Patrucco, "Structure-from-motion (Sfm) photogrammetry as a non-invasive methodology to digitalize historical documents: A highly flexible and low-cost approach?," *Heritage*, vol. 2, no. 3, pp. 2124–2136, 2019.

[17] J. Chen and K. C. Clarke, "Rapid 3d modeling using photogrammetry applied to google earth," *19th Int. Res. Symp. Comput. Cartogr. Albuquerque*, no. September 2016, pp. 14–16, 2016.

[18] H. K. Naser, F. M. Abed, and R. M. Hamdoon, "Preliminary quality assurance of printgrammetry technique-3D modeling from Google Earth 3D imagery data," *AIP Conf. Proc.*, vol. 2651, no. March, 2023.

[19] R. K. Horota *et al.*, "Printgrammetry: Google Earth Imagery Based 3D Model Generation for VR Applications," *Int. Geosci. Remote Sens. Symp.*, pp. 4292–4295, 2019.

[20] B. Alsadik, M. Gerke, and G. Vosselman, "Automated camera network design for 3D modeling of cultural heritage objects," *J. Cult. Herit.*, vol. 14, no. 6, pp. 515–526, 2013.

[21] G. Olague and E. Dunn, "Development of a practical photogrammetric network design using evolutionary computing," *Photogramm. Rec.*, vol. 22, no. 117, pp. 22–38, 2007.

[22] K. Kraus, *Photogrammetry Geometry from Images and Laser Scans*. Berlin, Boston: De Gruyter, 2015.

[23] H. H. Ali and F. M. Abed, "The impact of UAV flight planning parameters on topographic mapping quality control," *IOP Conf. Ser. Mater. Sci. Eng.*, vol. 518, no. 2, 2019.

[24] G. Guillet, T. Guillet, and L. Ravanel, "Camera orientation, calibration and inverse perspective with uncertainties: A Bayesian method applied to area estimation from diverse photographs," *ISPRS J. Photogramm. Remote Sens.*, vol. 159, pp. 237–255, 2020.

[25] C. Amrullah, D. Suwardhi, and I. Meilano, "Product Accuracy Effect of Oblique and Vertical Non-Metric Digital Camera Utilization in Uav-Photogrammetry To Determine Fault Plane," *ISPRS Ann. Photogramm. Remote Sens. Spat. Inf. Sci.*, vol. III–6, no. July, pp. 41–48, 2016.

[26] W. Ostrowski, "Accuracy of measurements in oblique aerial images for urban environment," *Int. Arch. Photogramm. Remote Sens. Spat. Inf. Sci. - ISPRS Arch.*, vol. 42, no. 2W2, pp. 79–85, 2016.

[27] C. S. Hsieh, D. H. Hsiao, and D. Y. Lin, "Contour Mission Flight Planning of UAV for Photogrammetric in Hillside Areas," *Appl. Sci.*, vol. 13, no. 13, 2023.

[28] M. Pepe, V. S. Alfio, and D. Costantino, "UAV Platforms and the SfM-MVS Approach in the 3D Surveys and Modelling: A Review in the Cultural Heritage Field," *Appl. Sci.*, vol. 12, no. 24, 2022.

[29] G. Gonçalves, D. Gonçalves, Á. Gómez-gutiérrez, U. Andriolo, and J. A. Pérez-alvárez, "3d reconstruction of coastal cliffs from fixed-wing and multi-rotor uas: Impact of sfm-mvs processing parameters, image redundancy and acquisition geometry," *Remote Sens.*, vol. 13, no. 6, 2021.

[30] W. Dai *et al.*, "Enhancing UAV-SfM Photogrammetry for Terrain Modeling from the Perspective of Spatial Structure of Errors," *Remote Sens.*, vol. 15, no. 17, pp. 1–19, 2023.

[31] Y. H. Tu *et al.*, "Combining Nadir, Oblique, and Façade Imagery Enhances Reconstruction of Rock Formations Using Unmanned Aerial Vehicles," *IEEE Trans. Geosci. Remote Sens.*, vol. 59, no. 12, pp. 9987–9999, 2021.